Three-dimensional solitons in coupled atomic-molecular Bose-Einstein condensates

T. G. Vaughan, K. V. Kheruntsyan, and P. D. Drummond

ARC Centre of Excellence for Quantum-Atom Optics, School of Physical Sciences, The University of Queensland, Brisbane, Queensland 4072, Australia

We present a theoretical analysis of three-dimensional (3D) matter-wave solitons and their stability properties in coupled atomic and molecular Bose-Einstein condensates (BECs). The soliton solutions to the mean-field equations are obtained in an approximate analytical form by means of a variational approach. We investigate soliton stability within the parameter space described by the atom-molecule conversion coupling, the atom-atom *s*-wave scattering, and the bare formation energy of the molecular species. In terms of ordinary optics, this is analogous to the process of sub- or second-harmonic generation in a quadratic nonlinear medium modified by a cubic nonlinearity, together with a phase mismatch term between the fields. While the possibility of formation of multidimensional spatiotemporal solitons in pure quadratic media has been theoretically demonstrated previously, here we extend this prediction to matter-wave interactions in BEC systems where higher-order nonlinear processes due to interparticle collisions are unavoidable and may not be neglected. The stability of the solitons predicted for repulsive atom-atom interactions is investigated by direct numerical simulations of the equations of motion in a full 3D lattice. Our analysis also leads to a possible technique for demonstrating the ground state of the Schrödinger-Newton and related equations that describe Bose-Einstein condensates with nonlocal interparticle forces.

I. INTRODUCTION

Recent developments in Bose-Einstein condensation of alkali-metal gases include the possibility of coherent molecule formation [1,2], or superchemistry [3] via Bose-enhanced chemical reaction at ultracold temperatures. The relevant parametric quantum field theories [1,2,4–6] and their classical nonlinear optical analogs [6–9] are the subject of much current attention, due to the possibility of stable, bright, higher-dimensional solitons (also referred to as solitary waves) [1,7,10,11]. Parametric solitons in nonlinear optics with quadratic nonlinearity have now been observed experimentally in two transverse dimensions, as both spatial and temporal solitons [12].

The dynamical equations for parametric solitons are an example of a classically nonintegrable field theory which generally needs to be treated numerically. The formation of three-dimensional (3D) localized solitons is a subject of much intrinsic interest in mathematical and nonlinear physics, and it is intriguing that no integrable models supporting them appear to exist. Despite the absence of integrability, the quadratically coupled equations of parametric nonlinear optics and coherently coupled atomic-molecular Bose-Einstein condensate (BEC) systems appear to be the simplest physically relevant Hamiltonian models having 3D localized solitons [13].

They also provide an experimental route toward demonstration of the closely related ground state of the Schrödinger-Newton (SN) equation [14] introduced to describe gravitationally bound Bose gases, and later revived by Penrose and others [15,16] as a possible model of the collapse of the quantum-mechanical wave function. We also show that there are parallels with more general mean-field models of Bose gases having a combination of short-distance repulsion and finite-range Yukawa-like attractive interac-tions. These more general models may also have astrophysical or quantum-mechanical significance.

The surprisingly close parallels to nonlinear optics, in the related fields of quantum many-body theory and atom optics, have now resulted in the emergence of a new field of research—nonlinear atom optics with parametric nonlinearity. The first step toward seeing molecular condensation was recently undertaken in transient experiments with a Bose-Einstein condensate of ^{85}Rb atoms [17], in which interference measurements were indicative of coherent molecule formation. More recent experiments with ^{133}Cs, ^{87}Rb, and ^{23}Na [18], as well as with degenerate Fermi gases of ^{40}K and ^{6}Li atoms [19], have produced even larger fractions of ultra-cold molecules, as well as Bose-Einstein condensates of bosonic molecular dimers composed of fermionic atoms. All these experiments have employed magnetic Feshbach resonances, which appear to be more successful at present than the alternative Raman photoassociation scheme [20].

In addition to this remarkable experimental progress, the original effective quantum field theory [1–6] for coupled atomic-molecular BECs has also been developed; it now incorporates renormalization, the treatment of intrinsic pair correlations, quantum fluctuations, and thermal effects (see, e.g., [21–29], as well as a recent review paper [30] for further references).

In the near-classical limit of large numbers of atoms or photons, the relevant equations for parametric solitons are those of mean-field theory, which is a modified version of the Gross-Pitaevskii (GP) equation (in the atomic BEC case) or the nonlinear Schrödinger equation (in the photonic case). These are in fact identical equations, except expressed in the different languages of condensed matter physics and photonics. The modification consists of the addition of a parametric nonlinear term analogous to a quadratic nonlinearity in nonlinear optics. This couples the atomic and molecular

fields together by means of a coherent interconversion process. The parametric coupling acts as an energy-lowering "glue," which can permit stable mutually trapped BEC solitons to form in 3D. In the absence of gravity, this would imply the possibility of localized matter waves in free space without external trapping potentials. Unlike the usual GP equations, the existence of attractive forces in three dimensions does not result in a catastrophic collapse, provided the s-wave scattering length is non-negative.

In nonlinear optics, various aspects of the competition between quadratic and cubic nonlinearities on soliton formation have been studied in Refs. [31], either in lower dimensions (1D or 2D) or in cases of special relations between the system parameters. Matter-wave solitons in 3D coupled atomic-molecular BECs have been studied in Refs. [1,6,11] and [32], but only for specific values of the s-wave couplings.

In the present paper, we extend these results to the case of arbitrary interaction strengths for the atom-molecule coupling and for the repulsive atom-atom s-wave scattering, as well as for arbitrary energy mismatch between the atoms and molecules. We analyze the superchemistry equations in the mean-field limit, to obtain the precise conditions under which 3D atomic-molecular BEC solitons can form. Approximate soliton solutions are found analytically, by means of a variational approach with a Gaussian and an exponential ansatz. We then numerically study the dynamical stability of the resulting solitons on a 3D lattice, together with comparing the results with exact numerical solutions.

We find that there are large regions of stability in parameter space, depending on the energy difference between the atomic and molecular condensates, the numbers of atoms involved, and the coupling strengths. For simplicity, the analysis only includes repulsive s-wave scattering between the atoms, and assumes no other s-wave interactions. While more general s-wave interactions are simple enough to include, we have focused on a relatively simple case here in the interest of keeping the parameter space manageable.

II. THE MODEL

We start with an effective field theory model for a coherently coupled atomic-molecular system [1]. The model and the obtained results can easily be adopted to describe certain cases of nonlinear optical interactions of second- and subharmonic waves in a nonlinear crystal [2,6]. In the atom-molecular case, the model refers to a type of superchemistry [3], in which an atomic condensate is able to coherently and reversibly interconvert with a condensate of diatomic molecules.

There are several possible experimental routes for providing this type of coherent coupling, including a Feshbach resonance (employing a tuned external dc magnetic field), Raman photoassociation (involving two external lasers with a well-defined frequency difference), and direct single-photon photoassociation (this would require an external microwave or infrared field) [1–5,21–30]. The first two cases have been experimentally demonstrated [17,20], although not yet the last. In practical terms, the main limitation of the

model and corresponding experiments is the need to minimize incoherent processes like inelastic collisions and other loss processes.

A. Hamiltonian

In the model, we suppose that each condensate has the usual kinetic energy term, atom-atom s-wave scattering interactions, and a number-conserving coherent coupling of the form $\hat{\Phi}^{\dagger}\hat{\Phi}^{\dagger}\hat{\Psi}$, where $\hat{\Phi}$ represents the atomic field, and $\hat{\Psi}$ is the field operator for the molecular dimers. In D ($D=1,2,3$) spatial dimensions, this leads to a model Hamiltonian of the following form:

$$
\begin{aligned}
\hat{H} = \int d^{D}\mathbf{x} \bigg[& \frac{\hbar^{2}}{2m_{1}} |\boldsymbol{\nabla}\,\hat{\Phi}(\mathbf{x})|^{2} + \frac{\hbar^{2}}{2m_{2}} |\boldsymbol{\nabla}\,\hat{\Psi}(\mathbf{x})|^{2} + V_{\Psi}\hat{\Psi}^{\dagger}(\mathbf{x})\hat{\Psi}(\mathbf{x}) \\
& + \frac{\hbar\kappa_{11}}{2}\hat{\Phi}^{\dagger}(\mathbf{x})\hat{\Phi}^{\dagger}(\mathbf{x})\hat{\Phi}(\mathbf{x})\hat{\Phi}(\mathbf{x}) - \frac{\hbar\chi}{2}[\hat{\Phi}^{\dagger}(\mathbf{x})\hat{\Phi}^{\dagger}(\mathbf{x})\hat{\Psi}(\mathbf{x}) \\
& + \hat{\Psi}^{\dagger}(\mathbf{x})\hat{\Phi}(\mathbf{x})\hat{\Phi}(\mathbf{x})] \bigg].
\end{aligned}
\tag{1}
$$

Here, m_{1} and m_{2} are the masses of the atoms and molecules, respectively, V_{Ψ} is the internal molecular energy relative to free atoms, and the coupling χ (which we assume is positive) describes coherent conversion of pairs of atoms into diatomic molecules, and vice versa. The atomic self-interaction strength κ_{11} is proportional to the s-wave scattering length. For example, in 3D, $\kappa_{11}=4\pi\hbar a_{11}/m_{1}$, where a_{11} is the atom-atom scattering length, which is assumed positive, as is usually needed to form a stable BEC in the first place.

To allow comparisons with the Schrödinger-Newton [14–16] equation, we will also consider a related model in which the interaction term $-\hbar\chi[\hat{\Phi}^{\dagger}\hat{\Phi}^{\dagger}\hat{\Psi}+\hat{\Psi}^{\dagger}\hat{\Phi}\hat{\Phi}]/2$ is replaced by $-\hbar\chi\hat{\Phi}^{\dagger}\hat{\Phi}[\hat{\Psi}+\hat{\Psi}^{\dagger}]/2$. This models a Bose-Einstein condensate $\hat{\Phi}(\mathbf{x})$ with short-range interactions, together with a long-range attractive force caused by the exchange of a mesonlike particle $\hat{\Psi}(\mathbf{x})$. In the mean-field theory limit, we call this model the Gross-Pitaevskii-Yukawa (GPY) model; it is more general than the Schrödinger-Newton model.

In astrophysical situations, the GPY mean-field theory reduces to the SN model in the combined limit of zero s-wave scattering, and an infinitely long-range gravitational interaction with $m_{2}\to 0$, leading to an inverse-square law [14]. The presence of a short-range interaction s-wave scattering term makes the GPY model more realistic than the usual SN model. The SN model is used to describe a degenerate Bose gas with gravitational self-interaction, and has also been suggested as a possible mechanism for wave-packet collapse in quantum mechanics [15,16]. In the one-dimensional case, the GPY theory is similar to the nonlinear interactions in an optical fiber caused by couplings of photons to phonons [33]. At the same time, the GPY model allows one to investigate attractive interactions with more general behavior than a simple inverse-square law.

At the quantum field level, either model Hamiltonian implicitly involves a δ-function effective interaction between the atoms, and so requires the use of a momentum cutoff

$k_{max} \ll 1/a_{11}$ for self-consistency. More rigorous regularization consists of renormalization of the theory [26] as $k_{max} \rightarrow \infty$. In the present paper, however, we employ a mean-field approximation, and restrict ourselves to the study of solitons that have spatial widths much larger than k_{max}^{-1} so that the cutoff dependencies are negligible, while the relevant parameters are the *observed* couplings. The mean-field theory is also a high-density approximation, since quantum fluctuations and correlations are expected to cause a quite different ground state to appear at low density [1,2,23,25].

A more complete model Hamiltonian should also incorporate atom-molecule and molecule-molecule s-wave scattering interactions. However, these greatly complicate the analysis, without adding much qualitatively new physics to the 3D soliton properties studied here. In addition, the respective scattering lengths are not known yet in most cases. For this reason, we assume that the atom-atom scattering is the dominant s-wave interaction and simply omit all other s-wave scattering processes, in the interest of simplicity.

B. Mean-field equations

The corresponding equations of motion for the mean fields in the atom-molecular model, following from the Hamiltonian (1) and valid at high densities, are

$$i\frac{\partial \phi(\mathbf{x},t)}{\partial t} = -\frac{\hbar}{2m_1}\nabla_{\mathbf{x}}^2\phi - \chi\phi^*\psi + \kappa_{11}|\phi|^2\phi,$$

$$i\frac{\partial \psi(\mathbf{x},t)}{\partial t} = -\frac{\hbar}{2m_2}\nabla_{\mathbf{x}}^2\psi + \Delta\omega\psi - \frac{1}{2}\chi\phi^2, \quad (2)$$

where $\hbar\Delta\omega = V_\psi$ is the energy mismatch on converting atoms to molecules, and $m_2 = 2m_1$.

In this model, the total number of particles N (i.e., the total number of atomic particles, including pairs of atoms inside the diatomic molecules) here is conserved:

$$N = N_1 + 2N_2 = \int d^D\mathbf{x}[|\phi(\mathbf{x},t)|^2 + 2|\psi(\mathbf{x},t)|^2]. \quad (3)$$

For completeness, we include the mean-field equations for the related GPY equations. These have the structure

$$i\frac{\partial \phi(\mathbf{x},t)}{\partial t} = -\frac{\hbar}{2m_1}\nabla_{\mathbf{x}}^2\phi - \frac{\chi}{2}\phi(\psi + \psi^*) + \kappa_{11}|\phi|^2\phi,$$

$$i\frac{\partial \psi(\mathbf{x},t)}{\partial t} = -\frac{\hbar}{2m_2}\nabla_{\mathbf{x}}^2\psi + \Delta\omega\psi - \frac{1}{2}\chi|\phi|^2. \quad (4)$$

In the limit of $m_2 \rightarrow 0$, $\chi \rightarrow \infty$, so that $\Delta\omega m_2 \rightarrow 0$ and $\chi^2 m_2 = 4\pi G m_1^2$, and assuming that ψ is real, we introduce a gravitational field potential $V_g = -\chi\psi$. In this long-range force limit, one can apply an adiabatic approximation to the second equation, which leads to the Poisson equation:

$$i\hbar\frac{\partial \phi(\mathbf{x},t)}{\partial t} = -\frac{\hbar^2}{2m_1}\nabla_{\mathbf{x}}^2\phi + V_g\phi + \hbar\kappa_{11}|\phi|^2\phi,$$

$$\nabla_{\mathbf{x}}^2 V_g = 4\pi G m_1^2|\phi|^2. \quad (5)$$

This can be recognized as the mean-field equation for a BEC having an additional self-gravitational force with the gravitational potential energy V_g and gravitational constant G, as well as the usual GP short-range interaction. Here, the conserved particle number is given by $N = \int d^3\mathbf{x}|\phi(\mathbf{x},t)|^2$. In the additional limit of $\kappa_{11} \rightarrow 0$, the equations correspond to the time-dependent version of the SN equation [14–16] in which there is no short-range self-interaction.

C. Dimensionless variables

1. Atom-molecular system

In general, atom-molecular solitons may exist with periodic phase and frequency ω, so that $i\partial\phi/\partial t = \omega\phi$ and $i\partial\psi/\partial t = 2\omega\psi$.

We introduce a characteristic time scale t_0 and a characteristic length scale $d_0 = \sqrt{\hbar t_0/2m_1}$. We also transform to dimensionless time and position variables,

$$\tau = t/t_0,$$

$$\xi_i = x_i/d_0 \quad (6)$$

and dimensionless fields,

$$u = \chi t_0 \phi e^{i\omega t},$$

$$v = \chi t_0 \psi e^{2i\omega t}. \quad (7)$$

This gives the corresponding equations of motion in dimensionless form, with no reduction in parameter space:

$$i\frac{\partial u}{\partial \tau} = -\nabla_{\xi}^2 u + \gamma_u u - u^* v + \alpha_{11}|u|^2 u,$$

$$i\frac{\partial v}{\partial \tau} = -\frac{1}{2}\nabla_{\xi}^2 v + \frac{\gamma}{2}v - \frac{1}{2}u^2. \quad (8)$$

Here we have introduced new dimensionless parameters according to

$$\alpha_{11} = \frac{\kappa_{11}}{\chi^2 t_0},$$

$$\gamma_u = -\omega t_0,$$

$$\gamma = (2\Delta\omega - 4\omega)t_0. \quad (9)$$

To make the scaling definite, we can set $\gamma_u = 1$ with no loss in generality, provided $\omega < 0$. This corresponds to a localized bound state with negative energy $E = \hbar\omega$; we do not investigate the unbound solutions here. The choice $\gamma_u = 1$ also gives a simple relationship between the dimensionless parameter γ and the detuning $\Delta\omega$,

$$\gamma = 4 + 2\Delta\omega t_0, \quad (10)$$

corresponding to a shifted energy mismatch.

For $\alpha_{11} = 0$ (and with an additional scaling of $u \rightarrow u/\sqrt{2}$), Eqs. (8) are equivalent to Eqs. (1) and (2) of Ref. [10], with the value of the coefficient $\delta = 1$. This corresponds to optical

parametric interaction in a quadratically nonlinear medium, in which the dispersion coefficients for the fundamental and second-harmonic fields are equal to each other.

We seek stationary solutions ($\partial u/\partial \tau = \partial v/\partial \tau = 0$) to the equations of motion (8), i.e., those that have

$$\nabla_\xi^2 u = u - u * v + \alpha_{11}|u|^2 u,$$

$$\nabla_\xi^2 v = \gamma v - u^2. \qquad (11)$$

These correspond to extrema of the following dimensionless atom-molecular Hamiltonian:

$$H^{(u,v)} = \int d^D\xi \left[|\nabla u|^2 + \frac{1}{2}|\nabla v|^2 + |u|^2 + \frac{\gamma}{2}|v|^2 - \frac{1}{2}[(u*)^2 v \right.$$
$$\left. + \text{c.c.}] + \frac{\alpha_{11}}{2}|u|^4 \right], \qquad (12)$$

where the expression for the original Hamiltonian energy in terms of the dimensionless variables is

$$H = \left(\frac{\hbar}{2m_1 t_0}\right)^{D/2} \frac{\hbar}{\chi^2} H^{(u,v)}. \qquad (13)$$

A conserved quantity for the (u,v) system, which is proportional to the total number of particles N, is

$$\mathcal{N}' = \int d^D\xi [|u(\xi,t)|^2 + 2|v(\xi,t)|^2]. \qquad (14)$$

2. Schrödinger-Newton system

Similarly, stationary solutions to the time-dependent SN equation (5) may also exist with frequency ω, so that $i\partial\phi/\partial t = \omega\phi$, with V_g following adiabatically. This translates Eq. (5) directly to the time-independent SN equation appearing in Refs. [14,16], for $\phi_s = \phi \exp(i\omega t)$:

$$\frac{\hbar^2}{2m_1} \nabla_{\mathbf{x}}^2 \phi_s = -E\phi_s + V_g \phi_s,$$

$$\nabla_{\mathbf{x}}^2 V_g = 4\pi G m_1^2 |\phi_s|^2, \qquad (15)$$

where $E = \hbar\omega$.

By introducing characteristic time and length scales, as in Eqs. (6), and transforming to dimensionless fields

$$u = t_0 \sqrt{2\pi G m_1} \phi_s,$$

$$v = -\frac{t_0}{\hbar} V_g, \qquad (16)$$

we obtain the dimensionless time-independent SN equations:

$$\nabla_\xi^2 u = u - vu,$$

$$\nabla_\xi^2 v = -u^2. \qquad (17)$$

The normalization is now given by $\int d^D\xi\, u^2 = |\mathcal{E}|^{-1/2}$. Here $\mathcal{E} = E/E_0$ is the dimensionless energy ($\mathcal{E} < 0$), and the energy scale E_0 is defined via $E_0 = 32\pi^2 m_1^5 N^2 G^2/\hbar^2$.

Note that Eqs. (17) are identical to Eqs. (11) for real stationary solutions to the atom-molecular system when $\gamma = \alpha_{11} = 0$.

III. VARIATIONAL ANALYSIS

A. Gaussian variational ansatz

To analyze the localized soliton solutions to Eqs. (8), where $\gamma_u = 1$, we introduce an approximate Gaussian variational ansatz (GVA). This permits an analytic treatment of the problem of minimizing the Hamiltonian energy. The stability of the GVA solutions will be checked numerically by dynamical evolution of the equations of motion where the GVA serves as the initial condition.

The GVA solutions are introduced according to

$$u(\xi, \tau = 0) = Ae^{-a\xi^2},$$

$$v(\xi, \tau = 0) = Be^{-b\xi^2}, \qquad (18)$$

where $\xi = |\xi|$. Here, the parameters a and b must both be real and positive for localized solitons, and we assume that both the amplitudes A and B are also real and positive. This choice in fact already takes care of the optimum relative phase between the atomic and molecular fields, where we can without loss of generality take B to be real, while the optimum relative phase will dictate the phase of A. This immediately leads us to the conclusion that A^2 must be real and positive too, in order that the atom-molecule interaction term remains negative (for positive χ as assumed here) and permits a minimum in the Hamiltonian energy. The sign of A is in fact irrelevant, since the corresponding equations of motion (8) are invariant under the sign change of A.

Substituting the GVA into Eqs. (14) and (12) for $\mathcal{N}'$ and the Hamiltonian energy $H^{(u,v)}$ and taking the integrals we obtain, in $D = 1, 2$, or 3 space dimensions:

$$\mathcal{N}' = \left(\frac{\pi}{2}\right)^{D/2} \left[\frac{A^2}{a^{D/2}} + \frac{2B^2}{b^{D/2}}\right], \qquad (19)$$

$$H^{(u,v)} = \frac{D}{2}\left(\frac{\pi}{2}\right)^{D/2} \left[\frac{2A^2}{a^{D/2-1}} + \frac{B^2}{b^{D/2-1}} + \frac{2A^2}{Da^{D/2}} + \frac{\gamma B^2}{Db^{D/2}} \right.$$
$$\left. - \frac{2^{1+D/2}A^2 B}{D(2a+b)^{D/2}} + \frac{\alpha_{11}A^4}{D(2a)^{D/2}}\right]. \qquad (20)$$

Minimizing $H^{(u,v)}$ with respect to a, b, A, and B (for given α_{11} and γ) gives the following solution:

$$a = \frac{b}{2}\left[\frac{2(Db+\gamma)}{(D-2)b+\gamma} - 1\right], \qquad (21)$$

$$\alpha_{11}(2a+b)^{1+D}(Db+\gamma)[(4-D)a-1] - 2^{1+D}(2ab)^{D/2}[4a^2$$
$$- (D-2)ab - b] = 0, \qquad (22)$$

$$B = \frac{(2a+b)^{D/2}(Da+1)}{(2a)^{D/2}}\left[1 - \frac{\alpha_{11}(2a+b)^D(Db+\gamma)}{2^D(2ab)^{D/2}}\right]^{-1}, \qquad (23)$$

$$A^2 = \frac{(2a+b)^{D/2}(Db+\gamma)}{(2b)^{D/2}}B. \tag{24}$$

In Eq. (22), the parameter a is to be substituted using Eq. (21), so that Eq. (22) (to be solved first) reads as a polynomial equation with respect to b, for given values of α_{11} and γ. Alternatively, b can be regarded as a free parameter and Eq. (22) be viewed and easily solved with respect to α_{11}, for given γ and b. In doing so, only positive b values have to be considered for physically meaningful (localized) soliton solutions.

For certain values of α_{11} and γ this system has a unique solution (see Sec. IV A, giving the soliton parameters A, B, a, and b. The soliton parameters give in turn the resulting value of the conserved quantity $\mathcal{N}'$, Eq. (19), and the Hamiltonian energy (20).

B. Exponential variational ansatz

It can be shown that any localized stationary solution to the equations of motion (8) (with $\gamma_u = 1$) must possess tails decaying according to

$$u(\xi \gg 1, \tau) \propto e^{-\xi}/\xi,$$

$$v(\xi \gg 1, \tau) \propto e^{-\sqrt{\gamma}\xi}/\xi, \tag{25}$$

where $\xi = |\xi|$. This result can be obtained by neglecting all nonlinear terms in Eqs. (8) at large ξ, and solving the resulting decoupled equations for the stationary states.

Due to the singularity at origin, direct employment of this variational trial function would be problematic. However, since it indicates that the soliton tails should decay more slowly than those of the Gaussian trial functions, we are motivated to also consider an alternative exponential variational ansatz (EVA):

$$u(\xi, \tau = 0) = P e^{-p\sqrt{\xi^2 + \varepsilon}},$$

$$v(\xi, \tau = 0) = Q e^{-q\sqrt{\xi^2 + \varepsilon}}. \tag{26}$$

As in the case of the GVA, here too we assume that p, q, P, and Q are all real and positive. For analytic simplicity, we let ϵ be an infinitely small length scale, which is formally included to ensure that u and v are differentiable at $\xi = 0$. We then proceed and evaluate the integrals in $\mathcal{N}'$ and $H^{(u,v)}$ to find that, as $\epsilon \to 0$:

$$\mathcal{N}' = K_D \left[\frac{P^2}{p^D} + \frac{2Q^2}{q^D} \right], \tag{27}$$

$$H^{(u,v)} = K_D \left[\frac{P^2}{p^{D-2}} + \frac{Q^2}{2q^{D-2}} + \frac{P^2}{p^D} + \gamma \frac{Q^2}{2q^D} - \frac{2^D P^2 Q}{(2p+q)^D} \right.$$
$$\left. + \alpha_{11} \frac{P^4}{2^{D+1}p^D} \right]. \tag{28}$$

Here, $K_D = 1$, $\pi/2$, π for $D = 1$, 2, 3, respectively.

Variational stationary points are then given by the solution to the following set of algebraic equations:

$$p = \frac{q}{2} \left[\frac{2D(q^2 + \gamma)}{(D-2)q^2 + D\gamma} - 1 \right], \tag{29}$$

$$2^{3D+1}(pq)^D \{ [(D-2)p^2 + D](2p+q) - 2Dp(p^2 + 1) \}$$
$$- \alpha_{11}(2p+q)^{2D+1}(q^2 + \gamma)[D - (4-D)p^2] = 0, \tag{30}$$

$$Q = \frac{[(D-2)p^2 + D](2p+q)^{D+1}}{D(2p)^{D+1}}$$
$$\times \left[1 - \alpha_{11} \frac{(q^2 + \gamma)(2p+q)^{2D+1}}{2^{3D+2}p^{D+1}q^D} \right]^{-1}, \tag{31}$$

$$P^2 = \frac{(q^2 + \gamma)(2p+q)^D}{(2q)^D} Q. \tag{32}$$

To compare the EVA solutions with those of the GVA, it is necessary to ensure that both have identical $\mathcal{N}'$ for a given pair of the parameters α_{11} and γ. As the solutions given above result from (unconstrained) variational minimization with respect to all parameters, this requirement will not in general be met. We thus perform a constrained minimization with respect to p, q, and Q, leaving P to be fixed by N′ of the associated GVA solution [34]. The constrained EVA solution for $D = 3$ is then given by

$$\frac{3}{8}\alpha_{11}pF - \frac{48pqQ}{(2p+q)^4} + 4 = 0, \tag{33}$$

$$F\left[\frac{3}{2}\alpha_{11}p^3Q + 48\frac{p^3q^4}{(2p+q)^4} \right] + 12Q\left[1 + p^2 - \frac{8p^3Q}{(2p+q)^3} \right]$$
$$- Q(3\gamma + q^2) = 0, \tag{34}$$

$$F\left[\alpha_{11}\frac{p^3}{q^3} + \frac{16p^3}{(2p+q)^3} \right] + \frac{8Q}{q^3}\left[1 + p^2 - \frac{8p^3Q}{(2p+q)^3} \right]$$
$$- \frac{2Q}{b}\left[1 + \frac{\gamma}{q^2} \right] = 0, \tag{35}$$

where we have defined $F \equiv \mathcal{N}'/\pi - 2Q^2/q^3$.

We note that a similar exponential variational solution for the "atomic" u field (though not for the "molecular" v field) has been used previously for the Schrödinger-Newton equation [16].

IV. 3D SOLITON PROPERTIES

A. Existence and properties of GVA solutions

In order to analyze the properties of the GVA solutions Eqs. (21)–(24), for a given pair of γ and α_{11}, we first note that our analysis is restricted to the case of $\alpha_{11} \geq 0$, i.e., repulsive atom-atom interactions including a noninteracting limit of $\alpha_{11} = 0$. In addition, we restrict ourselves to the three-dimensional case ($D = 3$) only.

Next, any localized physical solutions require a and b to be both real and positive. The existence of the minimum for the Hamiltonian energy, Eq. (20), requires that the product A^2B is real and positive too, so that the atom-molecule con-
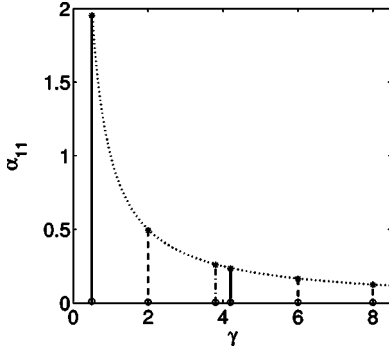
FIG. 1. GVA solutions existence domain in the (γ, α_{11}) plane, for $\gamma > 0$. The dotted line gives the upper bound on α_{11} corresponding to the boundary $\alpha_{11} < 1/\gamma$. The set of vertical lines in the region $\gamma < 4$ ($\gamma = 0.5$, full line; $\gamma = 2$, dashed line; and $\gamma = 3.8$, dash-dotted line), and in the region $\gamma > 4$ ($\gamma = 4.2$, full line; $\gamma = 6$, dashed line; and $\gamma = 8$, dash-dotted line) are to serve for mapping purposes as discussed in the text and explained in the captions to subsequent figures.

version term gives a negative contribution to the energy. As we mentioned earlier, this is achieved by taking both A and B to be positive.

To investigate the consequences of these requirements in terms of the soliton existence domain in the parameter space (α_{11}, γ), one has to start from solving numerically the polynomial Eq. (22). However, a simpler route that allows us to obtain analytical results is to view b as a free positive-valued parameter and solve Eq. (22) for α_{11} in terms of b and γ. In this case, the GVA solutions can be rewritten (for $D = 3$) in a simpler form:

$$a = \frac{b(5b + \gamma)}{2(b + \gamma)}, \tag{36}$$

$$\alpha_{11} = \frac{2^{4+3/2} a^{3/2} b^{3/2} (4a^2 - ab - b)}{(2a + b)^4 (3b + \gamma)(a - 1)}, \tag{37}$$

$$B = \frac{(2a + b)^{5/2}(a - 1)}{2^{3/2} a^{3/2}(b - 2a)}, \tag{38}$$

$$A^2 = \frac{(2a + b)^{3/2}(3b + \gamma)}{2^{3/2} b^{3/2}} B, \tag{39}$$

where we have substituted the solution for α_{11} into the expression for B, and the parameter a in Eqs. (37)–(39) is to be substituted using Eq. (36).

In Appendix A, we analyze the above set of equations for possible solutions. Restricting ourselves to the physically interesting subspace of $\gamma > 0$, we find that the soliton existence domain for the GVA is given by $0 \leq \alpha_{11} < 1/\gamma$. The parameter space identifying this in the (γ, α_{11}) plane is shown in Fig. 1. Here, the vertical lines at $\gamma = 0.5, 2, 3.8, 4.2, 6,$ and 8 serve as test lines for mapping purposes discussed in subsequent sections. The dotted line gives the upper bound on α_{11} corresponding to the boundary $\alpha_{11} < 1/\gamma$.
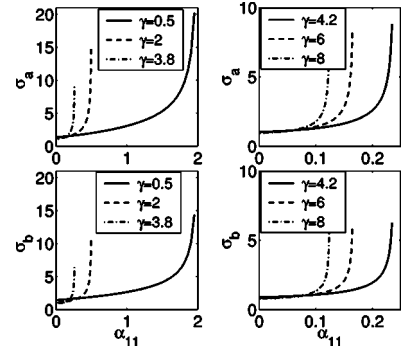

FIG. 2. GVA solution widths $\sigma_a = 1/\sqrt{2a}$ and $\sigma_b = 1/\sqrt{2b}$ as functions of α_{11}, for different values of γ corresponding to different vertical lines in Fig. 1.

Figure 2 represents the GVA soliton widths $\sigma_a = 1/\sqrt{2a}$ and $\sigma_b = 1/\sqrt{2b}$ as a function of α_{11} ($0 \leq \alpha_{11} < 1/\gamma$), for different values of γ. Similarly, Fig. 3 represents the fraction of the number of particles in the atomic field $\mathcal{N}_a'/\mathcal{N}'$ versus α_{11}, where $\mathcal{N}_a' = \int d^3\xi\, u^2$ is proportional to the total number of atoms, while $\mathcal{N}' = \int d^3\xi (u^2 + 2v^2)$ is proportional to the total number of atomic particles including pairs of atoms in the molecular component. Due to the conserved total particle number, the fraction of molecules is found from $\mathcal{N}_{mol}'/\mathcal{N}' = 0.5(1 - \mathcal{N}_a'/\mathcal{N}')$.

As we can see, for large negative detuning $\Delta\omega$, corresponding to $\gamma \ll 4$ ($\gamma > 0$), and for vanishing atom-atom repulsion ($\alpha_{11} \simeq 0$), the atomic fraction is relatively small and increases monotonically with increasing γ. In all cases, the atomic fraction decreases rapidly as α_{11} increases, due to the increased energy penalty resulting from interatomic interactions. The graphs for the soliton widths show that the atomic density profiles are in general wider than the corresponding molecular density profiles, and that the atomic component becomes wider and lower in the amplitude in the limit of strong interatomic repulsion, $\alpha_{11} \to 1/\gamma$. In this limit, it is energetically preferable for atom pairs to populate the molecular component so that the stable configuration of the system is a pure molecular condensate. We note that this is a consequence of the fact that our model neglects the molecule-molecule self-interaction completely.

B. Existence and properties of EVA solutions

Almost identical arguments relating to the soliton existence domain can be made for the EVA solutions. We again
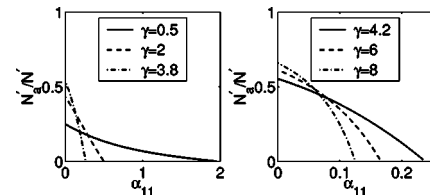

FIG. 3. Fraction of the number of particles in the atomic field $\mathcal{N}_a'/\mathcal{N}'$ for GVA solutions as a function of α_{11}, along the lines of fixed γ values as shown in Fig. 1.
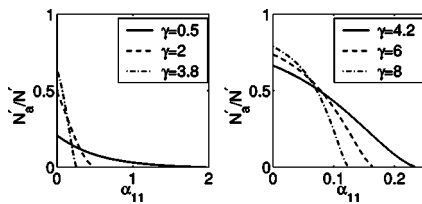
FIG. 4. Fraction of the number of particles in the atomic field $\mathcal{N}_a'/\mathcal{N}'$ for the EVA solutions as a function of α_{11}, along the lines of fixed γ values as shown in Fig. 1.

simplify the analysis by rewriting Eqs. (29)–(32) in the following form (for $D=3$):

$$p = \frac{q}{2}\left(\frac{5q^2 + 3\gamma}{q^2 + 3\gamma}\right), \tag{40}$$

$$\alpha_{11} = \frac{2^{10}p^3q^3[4p^3 - q(p^2 + 3)]}{(2p+q)^7(q^2+\gamma)(p^2-3)}, \tag{41}$$

$$Q = \frac{(2p+q)^4(p^2-3)}{3 \times 2^3 p^3(q - 2p)}, \tag{42}$$

$$P^2 = \frac{(2p+q)^3(q^2+\gamma)}{2^3 q^3}Q. \tag{43}$$

Here, the expression (41) for α_{11} is obtained from Eq. (30) and has been further substituted into Eq. (31) to obtain Eq. (42). The parameter p in Eqs. (41)–(43) is to be substituted using Eq. (40). By treating q as a free parameter instead of α_{11} (assuming $q > 0$ for localized solutions), we can first solve for p in terms of two independent parameters q and γ, and then proceed to find the remaining parameters, α_{11}, Q, and P.

In Appendix B, we analyze the above set of algebraic equations and conclude that for $\gamma > 0$ the existence domain for the EVA solutions is identical to that of the GVA solutions, and is given by $0 \leqslant \alpha_{11} < 1/\gamma$.

Figure 4 shows the dependence of the atomic number fraction $\mathcal{N}_a'/\mathcal{N}'$ for the EVA solution as a function of α_{11}, for various γ. As we see, the salient features of these curves, as well as the behavior of the EVA soliton widths, are similar to those of the GVA solutions discussed in the previous subsection.

V. DYNAMICAL STABILITY

In order for these variational solutions to prove useful, it is necessary to identify some correlation between their dynamical behavior and the existence of actual (exact) stable soliton solutions. To this end, we have identified the exact stationary solutions numerically, by means of the numerical relaxation method, and have checked their stability under dynamical evolution for a large number of test points in the $(\alpha_{11}\text{-}\gamma)$ parameter space within the GVA/EVA solutions existence domain, $0 \leqslant \alpha_{11} < 1/\gamma$ for $\gamma > 0$. What follows is an account of the dynamical behavior of the variational approximations, together with comparisons between this behavior and the existence of stable stationary points.
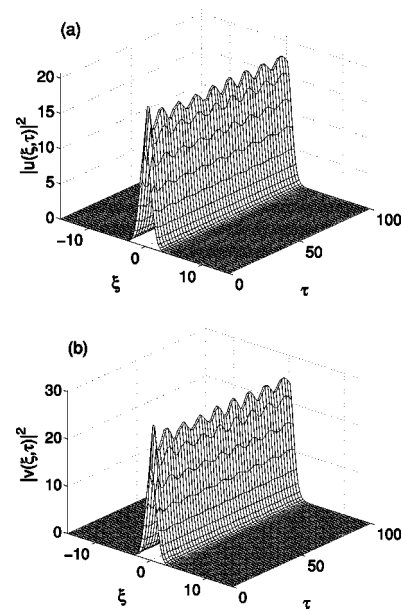

FIG. 5. Example of stable dynamical evolution of the GVA soliton. Shown are the particle number densities for the atomic (a) and molecular (b) fields for $\alpha_{11}=0.1$ and $\gamma=1$, with the GVA solution taken as the initial condition.

A. Stability of the GVA solutions

We have conducted a numerical analysis of the dynamics of the GVA solution for various (α_{11},γ) pairs lying within the existence domain $0 \leqslant \alpha_{11} < 1/\gamma$, for $\gamma > 0$. The details of this analysis are as follows.

We first used Eqs. (36)–(39) to obtain the parameters characterizing the GVA solution for each (α_{11},γ) pair in question. These solutions were then used, in conjunction with the dimensionless equations of motion (8), to form a set of initial value problems. The dynamical behavior of each Gaussian solution was then determined through numerical integration using a spherically symmetric [35] semi-implicit algorithm.

In Figs. 5–7 we show typical examples of the dynamical evolution of the atomic and molecular fields.

Figure 8 summarizes the results of our dynamical stability analysis, applied to many (α_{11},γ) pairs satisfying $\alpha_{11} \geqslant 0.01$, $\gamma \geqslant 0.01$, and $\alpha_{11} < 1/\gamma$. Here, the points marked with squares, circles, or crosses represent dynamics of the GVA solutions, which have been classified as stable, "oscillatory," or unstable in nature. (This necessarily involves a certain degree of ambiguity when distinguishing between the stable and oscillatory cases.) Here, the term oscillatory is used in a broad sense, and does not mean to imply true periodic oscillations around the original GVA solution or the exact stationary solution. The term unstable, on the other hand, refers to delocalization of the GVA solution over short time scales [36].

Remarkably, the GVA solutions display primarily stable dynamics within the $0 \leqslant \alpha_{11} < 1/\gamma$ parameter space. Exceptions to this are two regions close to the $\gamma=0.01$ axis. The lower of these regions (the shaded region in Fig. 8 containing circles) contains GVA solutions which, although remaining
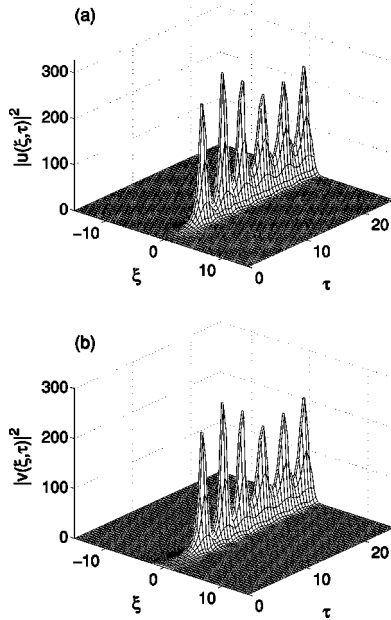
FIG. 6. Dynamical evolution of the atomic (a) and molecular (b) field densities for $\alpha_{11}=0.01$ and $\gamma=0.01$. This is an example representing strongly "oscillatory" behavior of the GVA solution.

localized, display highly oscillatory dynamics. Here, the EVA solutions have lower energy and give a better approximation to the exact solutions (see Sec. V C for further discussion). The other region contains unstable GVA solutions (marked by crosses) which delocalize rapidly under dynamical evolution.

We point out, however, that these regions are rather small in the physical parameter space (notice the logarithmic scale in Fig. 8). The most interesting area in this sense is about the $\gamma=4$ axis, corresponding to a minimum energy mismatch between the atomic and molecular fields, $\hbar\Delta\omega\simeq0$. For example, even for the detunings as large as $\Delta\omega\simeq-10^4$ s^{-1}, which gives an energy mismatch comparable in magnitude with typical mean-field energies in atomic Bose-Einstein condensates, the corresponding value of γ is of the order of $\gamma\simeq2$, for typical values of $N\simeq10^5$ and $\chi\simeq10^{-6}$ m$^{3/2}$/s (see also Sec. VI). In this physically interesting region, the GVA solutions are a good approximation to the exact solitons and maintain excellent dynamical stability.
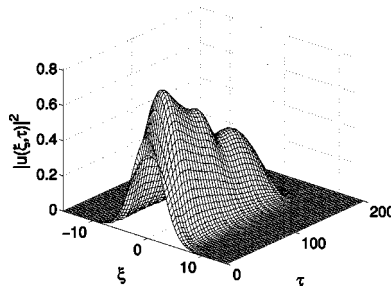

FIG. 7. Dynamical evolution of the GVA solution for $\alpha_{11}=3$ and $\gamma=0.01$ representing an example of unstable behavior. Shown is the particle number density for the atomic field, with similar behavior observed for the molecular field.
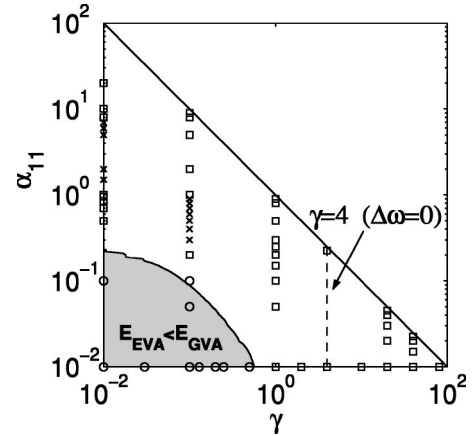

FIG. 8. Summary of the dynamical behavior of the GVA solutions for different (α_{11},γ) pairs. The squares, circles, and crosses indicate stable, strongly oscillatory, and unstable behavior, respectively. For discussion of the shaded region with $E_{EVA}<E_{GVA}$, see text in Sec. V C.

B. Existence of numerical exact solutions

By using the approximate GVA solution as an initial guess in the numerical relaxation algorithm, we have investigated the shape of the exact stationary solution having the same particle number as the GVA. This constraint is used to ensure that the numerically found exact solution corresponds to the same set of physical parameters as the GVA. The stability of each exact solution was determined in the same manner as that of the GVA, i.e., via real-time dynamical evolution governed by Eqs. (8). In all cases where a stationary solution was identified but found to be unstable, a modified initial guess was found that converged to a *stable* stationary solution. The modified Gaussian used in these cases was typically narrower and of higher peak density, while having the same total particle number. In a small subset of cases, no exact stationary solution was obtained (see below).

Figure 9 illustrates the time evolution of one such solution. This demonstrates the stability of the exact soliton solution, in contrast to those corresponding to energy maxima which become delocalized due to the buildup of small numerical inaccuracies such as rounding errors.
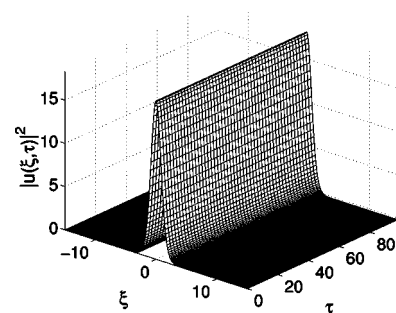

FIG. 9. Exact soliton dynamics with the exact solitary solution (found numerically) as the initial condition, for $\alpha_{11}=0.1$, $\gamma=1$, and $\mathcal{N}'$ being fixed to the same value as in the respective GVA solution. Shown is the particle number density for the atomic field, with similar behavior found for the molecular field.
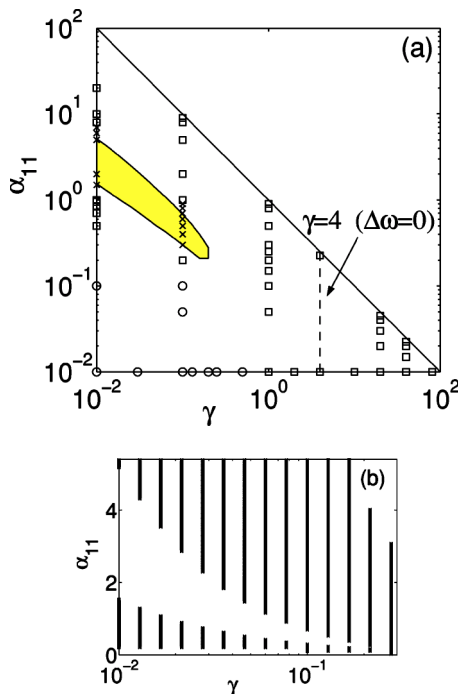
FIG. 10. (a) Comparison of stable soliton existence domain with the dynamical behavior of GVA solutions. Stable exact solutions were found for all marked points outside of the shaded region. The precise boundary of the shaded region, where no exact solutions were found, was identified by approaching it from below and from above along the vertical lines shown in (b). The lines themselves consist of points, of spacing 0.01 in α_{11}, for which the exact solutions were identified, while the interrupted part of each line corresponds to having no exact solutions.

In Fig. 10, we summarize the results of the stability analysis for the exact solutions and compare them with those of the GVA. Stable exact soliton solutions were identified for all (α_{11}, γ) pairs used in the GVA dynamical analysis (see Fig. 8), except those lying within the shaded region. The boundary of this region was found using an extra set of test points for higher accuracy. Distorting the initial guess input to the relaxation algorithm did not help in finding exact stable solutions in the shaded region. Note that, apart from a small number of exceptions near the boundary, all unstable GVA solutions in Fig. 8 which delocalized under dynamical evolution (as for the example in Fig. 7) are contained within the shaded region in Fig. 10. The physical origin of this instability is yet to be understood.

Thus, one can make the statement that the existence *and* dynamical stability of the GVA solution is strongly indicative of the existence of a true stationary soliton solution. This applies even to the case of strongly oscillatory GVA dynamics, in the sense that we were able to find a stable exact soliton solution whenever the oscillatory behavior of the GVA persisted for long evolution time.

C. Oscillatory dynamics and EVA solutions

Stationary solitons for (α_{11}, γ) pairs in the lower left corner of Fig. 8 are poorly approximated by the Gaussian ansatz
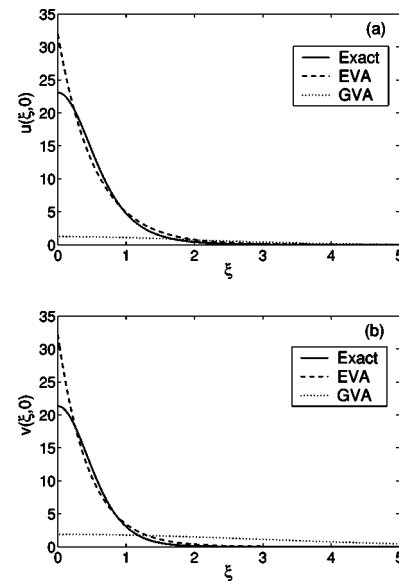

FIG. 11. Comparison of the density profiles for the atomic (a) and the molecular (b) fields described by the GVA, EVA, and exact stationary solutions, for $\alpha_{11}=0.01$ and $\gamma=0.01$. Note the dramatic failure of the GVA to approximate the exact solution in this case.

solutions—a fact revealed by the oscillatory GVA dynamics prevalent in this area. Examining the profiles of the corresponding numerically-obtained exact solutions suggests that the EVA solutions may provide a better approximation in this region.

In order to test this for a given (α_{11}, γ) pair, we need to ensure that the GVA and EVA solutions in question are being compared for the same value of the parameter $\mathcal{N}'$ corresponding to the total number of particles. Thus, we first identified the value of $\mathcal{N}'$ for the GVA solution, and then solved Eqs. (33)–(35) for the parameters of the corresponding *constrained* EVA solution.

Figure 11 illustrates the improvement in the fit of the profile of the EVA solution to that of the exact stationary solution, for $\alpha_{11}=\gamma=0.01$. The corresponding GVA solution is also shown for comparison. The resulting reduced amplitude of oscillation in the dynamics of the EVA is shown in Fig. 12.

In order to understand and quantify this improvement, the total Hamiltonian energy corresponding to both ansatz solutions has been calculated for a collection of points spanning the parameter space under consideration. The shaded area with $E_{EVA} < E_{GVA}$ in Fig. 8 represents the region of parameter space where the constrained EVA solutions have lower energy than that of the GVA. This analysis shows that the EVA indeed provides a better approximation to the exact solitons in cases when the dynamics of the GVA is strongly oscillatory.

Previous investigations of the SN equation [16], which has a stationary solution exactly equivalent to ours with $\gamma = \alpha_{11} = 0$, have come to the same conclusion that over a class of trial functions the exponential ansatz for the "atomic" field provides the best upper bound to the ground state energy. The fact that the upper bound provided by our solution, $-0.108 m^5 G^2 N^2/\hbar^2$, is higher than the value
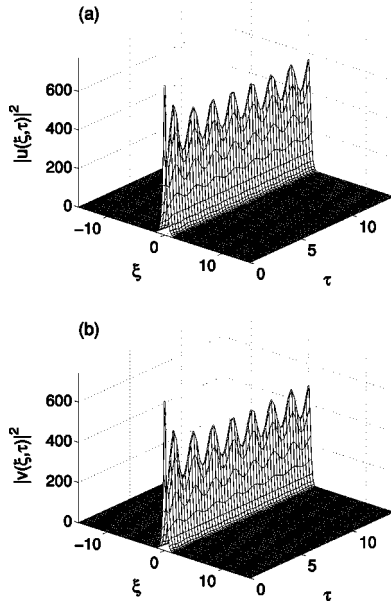
FIG. 12. Dynamical evolution of the EVA solution for α_{11} =0.01 and γ=0.01. Shown are the particle number densities for the atomic (a) and molecular (b) fields. This figure can be compared with the strongly oscillatory dynamics of the GVA solution in Fig. 6, and shows improvement in the stability of the EVA solution due to its lower energy.

$-0.146 m^5 G^2 N^2/\hbar^2$ quoted in [16] is due to the fact that we have used variational solutions for both u and v fields, rather than just for u. These upper bounds can be contrasted with the exact ground state energy of $-0.163 m^5 G^2 N^2/\hbar^2$ [14] which we have verified using our numerical relaxation code.

The SN helps to also understand the dramatic failure of the GVA solutions to approximate the exact solitons in the region of small γ and α. Here, the tails of the density distributions become increasingly important, and according to Eq. (25) the v field with $\gamma \to 0$ decays much slower than the tail of any Gaussian. In terms of the SN equation, this corresponds to evolution of the wave function in a very long-range potential v.

D. Energy surface topography

In order to better understand the nature of the instability marked by the shaded region in Fig. 10, it would be instructive to examine the topographical variations in the energy surface while approaching and crossing the boundary between the stable and the unstable regions. By tracing a single-dimensional trajectory between known critical points in the infinite dimensional coordinate space we can learn something of the higher-dimensional structure.

Figure 13 illustrates the topographical variation in the energy surface when the unstable region is approached from below as α_{11} is increased along the γ=0.01 line. Here, the critical points (including the unstable or delocalized solutions) for each (α_{11}, γ) pair were evaluated, and linear interpolation was used to generate a continuous path between stable (S), unstable (U) and delocalized (D) solutions, along a contour of constant $\mathcal{N}'$ [37].
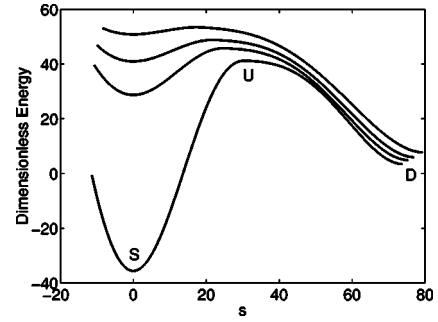

FIG. 13. Energy surface topography as one approaches the unstable region boundary from below along the γ=0.01 line. Shown is the dimensionless Hamiltonian energy vs the distance s in state space [37]. Different curves correspond (from bottom in increasing order) to α_{11}=0.2,0.5,0.7,1.

It is clear from this illustration that, as α_{11} approaches the unstable region, the soliton solution becomes metastable as it corresponds to a local rather than absolute minimum in the energy surface. This fact does not affect the existence of stable solutions, however, which persist until the local minimum is completely eliminated as the boundary is crossed into the unstable region.

We can use this analysis to explain the existence of GVA solutions which delocalize under evolution despite the existence of an exact stationary solution. In such cases, the width of the confining local minimum well (in state space) is smaller than the perturbation to the exact solution induced by enforcing the Gaussian ansatz. As one might expect, this only happens near a stability boundary, where the wells are small.

VI. RELATION TO PHYSICAL PARAMETERS

From the practical point of view, the question of interest is whether a given set of the physical parameters m_1, χ, κ_{11}, $\Delta\omega$, and the total number of particles N can support stable atomic-molecular solitons. In order to answer this question we must be able to interconvert between the soliton parameters in terms of the dimensionless variables and the original physical parameters. This procedure is not of a trivial matter, and requires a self-consistent solution that is able to map a given set of values of $(m_1, \chi, \kappa_{11}, \Delta\omega, N)$ into a pair of values of (γ, α_{11}), using the time scale t_0 and the length scale d_0. Depending on whether or not the pair of values of (γ, α_{11}) is inside the soliton existence domain $\gamma>0$ and $0 \leq \alpha_{11} < 1/\gamma$, one can then answer the above question and find the soliton parameter values in terms of dimensional variables, using the results of previous sections.

We recall that the relationships between the parameters of the dimensionless system and the original physical parameters are as follows:

$$\Delta\omega = (\gamma - 4)/2t_0, \tag{44}$$

$$\kappa_{11}/\chi^2 = \alpha_{11} t_0, \tag{45}$$

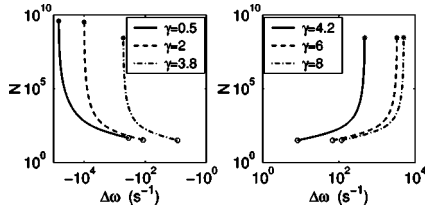$$N = \frac{1}{\chi^2 \sqrt{t_0}} \left(\frac{\hbar}{2m_1} \right)^{D/2} \mathcal{N}'. \tag{46}$$

FIG. 14. Variation in N and $\Delta\omega$ along the (α_{11}, γ) lines shown in Fig. 1. The values of the couplings χ and κ_{11} are held constant: $\chi = 10^{-6}$ m$^{3/2}$/s and $\kappa = 4.96 \times 10^{-17}$ m^3/s.

Here, the role of the mass m_1 is in setting up the length scale $d_0 = \sqrt{\hbar t_0 / 2m_1}$, so that the soliton widths are found unambiguously once the corresponding time scale t_0 is set up self-consistently. This leaves us, in general, with four independent variables $(\chi, \kappa_{11}, \Delta\omega, N)$ in the physical parameter space and two independent variables (γ, α_{11}) of the dimensionless system. Therefore, in order to be able to map the soliton existence domain in the (γ, α_{11}) plane into the physical parameter space, we have to restrict ourselves to cases where—out of four physical parameters $(\chi, \kappa_{11}, \Delta\omega, N)$—only two can be varied independently, while the other pair must be kept fixed.

Depending on which pair of the physical parameters is chosen to be fixed or varied, one can identify six different cases where the solution of the problem can be found unambiguously. As an example we consider the case where the fixed pair of the parameters are the couplings χ and κ_{11}, while the adjustable parameters are the detuning $\Delta\omega$ and the total number of particles N. This is the most physically relevant case, as the detuning and the total number of particles are easier to vary experimentally.

The procedure of mapping the soliton existence domain in the (γ, α_{11}) plane into the $(\Delta\omega, N)$ parameter space consists of solving Eqs. (44)–(46) to first identify t_0, using Eq. (45), and then finding the corresponding values of $\Delta\omega$ and N from the remaining two equations. As an intermediate step, this involves the evaluation of $\mathcal{N}' = \mathcal{N}'(\gamma, \alpha_{11})$ using Eq. (19), where the soliton parameters a, b, A, and B are found from the GVA solutions for the (γ, α_{11}) pair in question. Figure 14 demonstrates this mapping for the values of κ_{11} and χ typical of a ^{87}Rb BEC experiments.

Similar mapping can easily be constructed in other cases, where depending on the choice of the fixed pair of the physical parameters the sequential order of solving Eqs. (44)–(46) will vary. In all cases, the initial step should consist of identifying the value of the "dummy" parameter t_0 using one of the equations (44)–(46), and then eliminating it in favor of the remaining pair of the physical parameters in question.

VII. SUMMARY

To summarize, we have applied both Gaussian and exponential variational approximations to the problem of identifying 3D soliton solutions to parametrically coupled dilute atomic and molecular Bose condensates, with atomic self-interaction present. The soliton existence domain has been investigated, and for $\gamma > 0$ found to be defined by $0 \leqslant \alpha_{11} < 1/\gamma$ in both cases.

A detailed numerical study of the dynamical behavior of the Gaussian ansatz solutions has revealed that, as a rule of thumb, localized propagation of GVA solutions indicates the existence of true (and stable) stationary solutions. Furthermore, in regions where the GVA propagation is strongly oscillatory, the corresponding exponential ansatz solutions have been found to possess a lower energy, and propagate almost without oscillations. This indicates that systems for which the energy of molecular formation is large and negative and which have weak atomic self-interaction possess stationary solutions better approximated by the exponential rather than Gaussian ansatz. Finally, we have identified an anomalous instability "island" in the (α_{11}, γ) parameter space, where the Gaussian solitons were dynamically unstable *and* where no exact stationary solutions were numerically found.

The results obtained give the precise conditions under which 3D coupled atomic-molecular BEC solitons can form. This is done in terms of the dimensionless parameters (α_{11}, γ) that originate from physical parameters determined by the atom-molecule coupling, atom-atom repulsive s-wave scattering, and the energy detuning between the atomic and molecular fields. The total number of particles N in the system is incorporated in the analysis self-consistently, via scaling with respect to the time scale t_0 or equivalently with respect to the choice of the energy origin. We have shown how one can in principle map the physical parameter space into the parameter space defined by the dimensionless parameters (α_{11}, γ), and hence identify whether a particular set of physical parameter values $(\chi, \kappa_{11}, \Delta\omega, N)$ lies within the identified soliton existence and stability domain in the (α_{11}, γ) plane.

Beyond the theoretical interest, the realization of this type of coupled BEC soliton could provide a way to stabilize the otherwise diverging output of an atom-molecular laser, providing a technique for delivering a localized, intense, and coherent atomic-molecular field to a target or a detector.

The steady-state and variational solutions found here are also applicable to generalizations of the Schrödinger-Newton equation.

APPENDIX A

Standard algebraic analysis of Eqs. (36)–(39) for possible solutions, for a given pair of $\alpha_{11} \geqslant 0$ and γ, gives the following results. First of all, it is easy to see that for $b > 0$ and $B > 0$, the requirement $a > 0$ and $A^2 > 0$ (so that $A^2 B > 0$ too) can be satisfied only if $\gamma + b > 0$. From this, it also follows that $3b + \gamma > 0$, $5b + \gamma > 0$, and $b - 2a < 0$. Next, one can easily see that $B > 0$ if $a - 1 < 0$. This last inequality can be solved in terms of b, giving the result that b must satisfy $b < b_1$, where

$$b_1 = \frac{1}{10}[(2-\gamma) + \sqrt{(2-\gamma)^2 + 40\gamma}] \qquad (A1)$$

corresponds to the positive-valued solution of the quadratic equation for b which follows from $a-1=0$. Thus, as long as $0 < b < b_1$ ($a-1<0$) and $\gamma+b>0$, we satisfy the requirements that $a>0$, $B>0$, and $A^2>0$.

Analysis of the remaining requirement of $\alpha_{11} \geq 0$ is now reduced to the solution of $4a^2 - ab - b \leq 0$, within the region $0 < b < b_1$ (where $a-1<0$) and for $\gamma+b>0$. Here one has to distinguish and consider separately two cases corresponding to $\gamma \leq 0$ and $\gamma > 0$.

For $\gamma \leq 0$ the analysis is quite complicated and requires a pure numerical investigation. The overall conclusion is that the soliton existence domain is now restricted to a very small region which is not of major physical interest. For example, for $\alpha_{11}=0$, this domain is limited to the values of γ within a narrow interval $-0.0074 < \gamma \leq 0$. The size of this interval decreases with increasing α_{11} and approaches $-1/\alpha_{11} < \gamma < 0$ as $\alpha_{11} \to \infty$. In terms of the original (physical) phase mismatch parameter $\Delta\omega$, a physically interesting and important region corresponds to the values of $\Delta\omega \simeq 0$ which we note correspond to $\gamma \simeq 4$, while $\gamma < 0$ corresponds to very large and negative detuning $\Delta\omega$. For this reason, in the remaining of the paper we only treat the case of $\gamma > 0$.

For $\gamma > 0$ we proceed with the analytic treatment as follows. Substituting a from Eq. (36), one can rewrite the inequality $4a^2 - ab - b \leq 0$ (equivalent to $\alpha_{11} \geq 0$) in the following form

$$45b^2 + (14\gamma - 2)b + \gamma(\gamma-4) \leq \frac{2\gamma^2}{b}. \qquad (A2)$$

Taking here the equality sign, and considering the left and the right hand sides as functions of b, gives an equation that can always be solved graphically, with the result that for $\gamma > 0$ there always exists one and only one real *positive* solution for b, which we define via b_0. Consequently, the above inequality and therefore $\alpha_{11} \geq 0$ is satisfied if $0 < b \leq b_0$.

The next step in our analysis consists of showing that $b_0 < b_1$, thus restricting the soliton existence region to $0 < b \leq b_0$ from which it follows that for $\gamma > 0$ the requirements $a>0$, $\alpha_{11} \geq 0$, $B>0$, and $A^2>0$ are satisfied simultaneously. The proof of $b_0 < b_1$ is accomplished by first noting that $b=b_1$ (corresponding to $a-1=0$) is the pole of α_{11}, and that α_{11} is a continuous single-valued function of b within the interval $0 < b \leq b_1$. The discontinuity at $b=b_1$ is such that $\alpha_{11} \to -\infty$ as $b \to b_1 - 0$ and $\alpha_{11} \to +\infty$ as $b \to b_1 + 0$. In addition, $\lim_{b\to 0}\alpha_{11} = 1/\gamma > 0$, and since b_0 is the only positive root of the cubic equation (A2), we conclude that the crossover ($b=b_0$) of α_{11} from positive to negative values can only take place at $b < b_1$, which implies that $b_0 < b_1$.

Finally, one can show graphically (see Fig. 15), that within the interval $0 < b \leq b_0$ and for $\gamma > 0$, α_{11} is a monotonically decreasing function of b. It approaches its maximum $\alpha_{11} \to 1/\gamma$ as $b \to 0$, and $\alpha_{11}=0$ at $b=b_0$. This implies that there is one-to-one correspondence between the soliton existence domain $0 < b \leq b_0$ and the interval $0 \leq \alpha_{11} < 1/\gamma$,
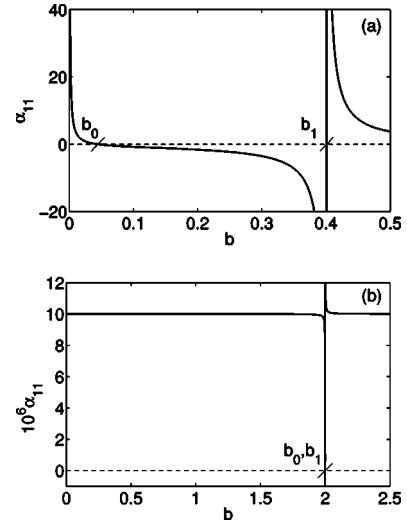

FIG. 15. The variation in α_{11} as a function of b, for $\gamma=0$ (a) and (b) 10^5, illustrating that α_{11} is monotonically decreasing function of b on $0 < b \leq b_q$.

for $\gamma > 0$. In other words, the interval $0 \leq \alpha_{11} < 1/\gamma$ ($\gamma > 0$) can be equally regarded as the soliton existence domain in the parameter space (α_{11}, γ).

APPENDIX B

Here we analyze the set of algebraic equations (40)–(43) for possible solutions for a given pair of $\alpha_{11} \geq 0$ and γ, with p, q, P, and Q all being real and positive. The analysis is very similar to the one carried out for the GVA solutions, and we summarize it as follows.

For $q > 0$ (as required), in order that $p > 0$ it is clearly necessary that $q^2 + 3\gamma > 0$, since in this case we also have $5q^2 + 3\gamma > 0$. In addition, for P^2 to be positive one has to have $q^2 + \gamma > 0$, provided that $Q > 0$ (as required). The condition $q^2 + 3\gamma > 0$ then leads to the requirement that $p^2 - 3 < 0$ for Q to be indeed positive, since $q^2 + 3\gamma > 0$ and $q > 0$ imply that $q - 2p < 0$.

Substituting the expression for p into $p^2 - 3$, the requirement $p^2 - 3 < 0$ can be written in the form

$$25q^6 + (30\gamma - 12)q^4 + (9\gamma^2 - 72\gamma)q^2 - 108\gamma^2 < 0. \qquad (B1)$$

It is clear that, as the left hand side of the inequality is a polynomial of even order, it can be satisfied if its largest real root q_1 is positive. By performing a numerical analysis of this polynomial, we find that real positive solutions exist for all γ, and that $q_1 \to 2\sqrt{3}$ as $\gamma \to \infty$. As in the case of the GVA solutions, we restrict ourselves to the physically interesting subspace of $\gamma > 0$. In this case, there always exist one and only one real positive solution q_1 to the above polynomial. Thus, provided $0 < q < q_1$ (i.e., $p^2 - 3 < 0$) and $q^2 + 3\gamma > 0$, the requirements that $p > 0$, $Q > 0$, and $P > 0$ are met.

Turning to the remaining equation for α_{11}, Eq. (41), with $\alpha_{11} \geq 0$, we next find that we must have $4p^3 - q(p^2+3) \leq 0$ (in conjunction with $p^2 - 3 < 0$) on the domain $0 < q < q_1$. Here,
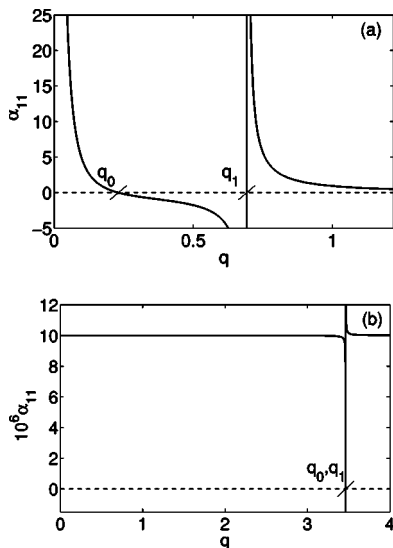
FIG. 16. The variation in α_{11} as a function of q, for $\gamma=0$ (a) and (b) 10^5. Note that $q_0 < q_1$ and that $q_0, q_1 \to 2\sqrt{3}$ for large γ.

we have also taken into account the fact that the term $(q^2 + \gamma)$ is always positive, for $\gamma > 0$. Substituting the expression for p from Eq. (29) into $4p^3 - q(p^2+3) \leq 0$ we find that this inequality is equivalent to

$$241q^8 + (345\gamma - 12)q^6 + \gamma(171\gamma - 108)q^4 + \gamma^2(27\gamma - 324)q^2 - 324\gamma^3 \leq 0, \tag{B2}$$

and can be satisfied if the largest real root q_0 to the polynomial in the left hand side is positive. We again employ numerics to find that for $\gamma > 0$ there exist only one real and positive root q_0, i.e., the above inequality is satisfied for q on $0 < q \leq q_0$. In the limit of large γ, $q_0 \to 2\sqrt{3}$.

Finally, as for the GVA solutions, we can show numerically (see Fig. 16) that α_{11} is a monotonically decreasing function of q on $0 < q < q_0$, and that $q_0 < q_1$. It approaches its maximum value $1/\gamma$ as $q \to 0$, and $\alpha_{11}=0$ at $q=q_0$. This implies that there exists one-to-one correspondence between the intervals $0 < q \leq q_0$ and $0 \leq \alpha_{11} < 1/\gamma$ ($\gamma > 0$), so that the latter can equally be regarded as the soliton existence domain for the EVA solutions on the parameter space (α_{11}, γ).

[1] P. D. Drummond, K. V. Kheruntsyan, and H. He, Phys. Rev. Lett. **81**, 3055 (1998).

[2] K. V. Kheruntsyan and P. D. Drummond, Phys. Rev. A **58**, R2676 (1998); **58**, 2488 (1998).

[3] D. J. Heinzen, R. H. Wynar, P. D. Drummond, and K. V. Kheruntsyan, Phys. Rev. Lett. **84**, 5029 (2000).

[4] E. Timmermans et al., Phys. Rev. Lett. **83**, 2691 (1999); Phys. Rep. **315**, 199 (1999).

[5] J. Javanainen and M. Mackie, Phys. Rev. A **59**, R3186 (1999).

[6] K. V. Kheruntsyan and P. D. Drummond, Phys. Rev. A **61**, 063816 (2000).

[7] A. A. Kanashov and A. M. Rubenchik, Physica D **4**, 122 (1981).

[8] M. Hillery and L. D. Mlodinov, Phys. Rev. A **30**, 1860 (1984).

[9] M. G. Raymer, P. D. Drummond, and S. J. Carter, Opt. Lett. **16**, 1189 (1991); P. D. Drummond and M. Hillery, Phys. Rev. A **59**, 691 (1999).

[10] B. A. Malomed, P. D. Drummond, H. He, A. Berntson, D. Anderson, and M. Lisak, Phys. Rev. E **56**, 4725 (1997).

[11] P. D. Drummond, K. V. Kheruntsyan, and H. He, J. Opt. B: Quantum Semiclassical Opt. **1**, 387 (1999).

[12] X. Liu, L. J. Qian, and F. W. Wise, Phys. Rev. Lett. **82**, 4631 (1999); X. Liu, K. Beckwitt, and F. Wise, Phys. Rev. E **61**, R4722 (2000).

[13] If the requirement of localization (relative to a vanishing background) is dropped, there is another possibility: Topological 3D solitons that require an infinite background of a uniform BEC have been shown to exist in spinor condensates; see: J. Ruostekoski and J. R. Anglin, Phys. Rev. Lett. **86**, 3934 (2001); C. M.Savage and J. Ruostekoski, ibid. **91**, 010403 (2003); J. Ruostekoski, Phys. Rev. A **70**, 041601 (2004).

[14] R. Ruffini and S. Bonazzola, Phys. Rev. **187**, 1767 (1969).

[15] R. Penrose, Philos. Trans. R. Soc. London, Ser. A **356**, 1927 (1998); I. Moroz, R. Penrose, and K. P. Tod, Class. Quantum Grav. **15**, 2733 (1998).

[16] K. P. Todd, Phys. Lett. A **280**, 173 (2001).

[17] E. A. Donley et al., Nature (London) **417**, 529 (2002).

[18] J. Herbig et al., Science **301**, 1510 (2003); K. Xu et al., Phys. Rev. Lett. **91**, 210402 (2003); S. Dürr et al., ibid. **92**, 020406 (2004).

[19] C. A. Regal et al., Nature (London) **424**, 47 (2003); M. Greiner et al., ibid. **426**, 537 (2003); K. J. Cubizolles et al., Phys. Rev. Lett. **91**, 240401 (2003); K. E. Strecker et al., ibid. **91**, 080406 (2003); M. W. Zweirlein et al., ibid. **91**, 250401 (2003).

[20] R. H. Wynar et al., Science **287**, 1016 (2000).

[21] F. A. van Abeelen and B. J. Verhaar, Phys. Rev. Lett. **83**, 1550 (1999).

[22] V. A. Yurovsky, A. Ben-Reuven, P. S. Julienne, and C. J. Williams, Phys. Rev. A **60**, R765 (1999).

[23] M. Holland, J. Park, and R. Walser, Phys. Rev. Lett. **86**, 1915 (2001).

[24] K. Góral, M. Gajda, and K. Rzażewski, Phys. Rev. Lett. **86**, 1397 (2001).

[25] J. J. Hope and M. K. Olsen, Phys. Rev. Lett. **86**, 3220 (2001).

[26] S. J. J. M. F. Kokkelmans and M. J. Holland, Phys. Rev. Lett. **89**, 180401 (2002).

[27] M. Mackie, K. A. Suominen, and J. Javanainen, Phys. Rev. Lett. **89**, 180403 (2002).

[28] T. Köhler, T. Gasenger, and K. Burnett, Phys. Rev. A **67**, 013601 (2003).

[29] R. A. Duine and H. T. C. Stoof, J. Opt. B: Quantum Semiclassical Opt. **5**, 212 (2003); Phys. Rev. Lett. **91**, 150405 (2003).

[30] R. A. Duine and H. T. C. Stoof, Phys. Rep. **86**, 115 (2004).

[31] A. V. Buryak, Yu. S. Kivshar, and S. Trillo, Opt. Lett. **20**, 1961 (1995); M. A. Karpierz, ibid. **20**, 1677 (1995); S. Trillo,

A. V. Buryak and Yu. S. Kivshar, Opt. Commun. **122**, 200 (1996); O. Bang, J. Opt. Soc. Am. B **14**, 51 (1997); L. Bergé, O. Bang, J. J. Rassmussen, and V. K. Mezentsev, Phys. Rev. E **55**, 3555 (1997); O. Bang, Yu. S. Kivshar, A. V. Buryak, A. De Rossi, and S. Trillo, *ibid.* **58**, 5057 (1998).

[32] B. J. Cusack, T. J. Alexander, E. Ostrovskaya, and Y. Kivshar, Phys. Rev. A **65**, 013609 (2002).

[33] S. J. Carter and P. D. Drummond, Phys. Rev. Lett. **67**, 3757 (1991).

[34] The total number of particles $\mathcal{N}' = \mathcal{N}'(P, Q, p, q)$ is a single-valued function of the EVA variables, and each of these variables can be treated as a single-valued function of $\mathcal{N}'$ and the three remaining variables. Because of this, the specific choice of the variables used here for the constrained minimization [relying on the elimination of P in favor of $\mathcal{N}'$, via $P^2 = p^3(\mathcal{N}'/\pi - 2Q^2/q^3)$] is just a matter of convenience and appears to be the simplest.

[35] Calculations with enforced spherical symmetry were used only after ensuring that the full 3D lattice simulations give identical results, which was verified for a smaller set of test points in the $(\alpha_{11} - \gamma)$ parameter space.

[36] The relevant time scales for dynamical stability of the soliton solutions, for each pair of the parameters α_{11} and γ, are determined by comparing the results with those observed for the case when the nonlinear coupling terms are removed from the equations of motion.

[37] For example, defining vectors $\vec{u} = (u, \sqrt{2}v)$, we interpolate between stable and unstable solutions $\vec{u}_S$ and $\vec{u}_U$ by first setting $\vec{u}'_\nu = \vec{u}_S + \nu(\vec{u}_U - \vec{u}_S)$ where ν runs from 0 to 1 and then normalizing so that $\vec{u}_\nu = \sqrt{\mathcal{N}'}\vec{u}'_\nu/|\vec{u}'_\nu|$. The variable s is an arclength defined as $s(\vec{u}_\nu) = \sqrt{\mathcal{N}'}\cos^{-1}(|\vec{u}_\nu \cdot \vec{u}_S|/\mathcal{N}')$. Here, inner products are defined as $\vec{u}_1 \cdot \vec{u}_2 = 4\pi \int dr\, r^2(u_1^* u_2 + 2v_1^* v_2)$ so that $\vec{u} \cdot \vec{u} = \mathcal{N}'$.

[38] http://www.xmds.org